



Published in final edited form as:

J Fluoresc. 2004 July ; 14(4): 417–423.

Fluorescence Enhancements on Silver Colloid Coated Surfaces

Joanna Lukomska¹, Joanna Malicka¹, Ignacy Gryczynski¹, and Joseph R. Lakowicz^{1,2}

¹ Department of Biochemistry and Molecular Biology, Center for Fluorescence Spectroscopy, University of Maryland at Baltimore, 725 West Lombard Street, Baltimore, Maryland 21201

Abstract

We observed a strong, more than 16-fold, enhancement of Texas Red-labeled BSA fluorescence emission when deposited on silver colloid coated surfaces (SCCS). The same labeled protein deposited on silver island films (SIFs) showed an approximate 8-fold fluorescence enhancement. The lifetimes of Texas Red-BSA fluorescence are significantly shorter on silvered surfaces than on uncoated quartz substrate indicating a strong change in radiative decay rate of the dyes. We also observed a 36-fold increased brightness of overlabeled fluorescein-HSA deposited on silver colloid coated surface. Stronger enhancement observed for overlabeled FI-HSA protein indicates that presence of silver particles partially decreased self-quenching. Our results indicate that surfaces coated with silver colloids are valuable substrates for metal-enhanced fluorescence.

Keywords

Silver island films; colloids; metal-enhanced fluorescence

Introduction

The influence of metallic surfaces on a dye emission has been already reported three decade ago by Drexhage [1]. The observed oscillations of lifetimes with distance in front of a mirror can be explained by changes in the phase of the reflected light field with distance [2]. The decreased emission rate of fluorophores between closely spaced mirrors was observed and interpreted as effects in cavity quantum electrodynamics [3–5]. The effects of metallic surfaces on optical properties of molecules depend on the nature of the metal surface. Much stronger effects are observed for roughened than smooth surfaces. The Raman signals, for example, are many orders of magnitude enhanced by metallic colloid or islands [6,7] which resulted in a new technology called surface enhanced Raman spectroscopy (SERS). The effects of silver islands on fluorescence were studied experimentally [8–10] and theoretically [11,12] in the 1980's. More recent studies include two-photon excitation near metallic particles [13–15], emission near roughened electrodes [16], light deposited silver [17], deposited colloids [18] and silver fractals [19,20]. The increased brightness of the dyes near silver islands enables the measurements of the DNA hybridization kinetics [21]. In several systems improvements in the fluorophore photostability near silver particles have been reported [16,22,23]. The combination of increased brightness, shorter lifetime and better photostability makes the metal enhanced emission an attractive tool in miniaturized sensing devices development. Therefore there is a constant need for a development and characterization of metallic surfaces which provide the largest enhancement in fluorescence. In this manuscript we compare the enhancements observed for silver island films (SIFs) and silver colloid coated surfaces (SCCS).

² To whom correspondence should be addressed. lakowicz@cfs.umbi.umd.edu.

Materials and Methods

Silver Films Preparation

Silver Island Film (SIF)—The quartz slides used for silver deposition were first cleaned overnight by soaking in 10:1 (v/v) mixture of H₂SO₄ (95–98%) and H₂O₂ (30%). Use of this cleaning solution requires extreme caution to avoid organic materials. After washing with ultrapure water, the quartz surface was coated with amino groups by dipping the slides in a 1% aqueous solution of 3-aminopropyltriethoxysilane (APS) for 30 min at room temperature. The slides were washed extensively with water and air-dried. Silver island film (SIF) deposition was accomplished as described previously [13–15]. Briefly, ten drops of fresh 5% NaOH solution were added to a stirring silver nitrate solution (0.25 g in 35 mL of water). 1 mL of ammonium hydroxide was added drop by drop to redissolved the dark-brown precipitate. The solution was cooled to 5°C in an ice bath and a fresh solution of D-glucose (0.36 g in 10 mL of water) was added, followed by placing two pairs of APS-coated quartz slides into the solution. The mixture was stirred for 2 min in ice bath and then allowed to warm up to 30°C for the next 5 min. As the color of the mixture turned from yellow-greenish to yellow-brown the color of the slides became greenish. The slides were removed from the beaker, rinsed with water and bath sonicated for 1 min at room temperature. Only one side of each slide was coated with silver islands.

Silver Colloid Coated Surfaces (SCCS) [24]—To a stirred solution of AgNO₃ (36 mg in 200 mL H₂O) at 60°C 4 mL trisodium citrate (34 nM) was added dropwise. The reaction mixture was warmed to 87–90°C and stirring was continued for 1 hr (until color of reaction mixture turned to an orange-greenish). Resulting mixture was then cooled in ice-water bath for 20 min. The colloid was purified by centrifugation 9000 rpm for 8 min and the precipitate (residue) was dissolved in 1 mM trisodium citrate (10 mL). Finally, two APS-coated quartz slides were immersed in colloid and allowed to stay in darkness at 4°C for 18 hr. After taking of quartz slides from tube with colloid we observed two types of surfaces. First layer, which was immersed deeper, had yellow color, and second above the yellow one had grey. In this paper SCCS is applied to the grey part.

Comparison of SIFs and SCCs—In order to compare the enhancement properties of SIFs and SCCS we deposited a similar densities of both on the quartz slides. Figure 1 shows absorption spectra of SIFs (top), yellow type (middle) and SCCS (bottom). A broad absorption spectrum of SIFs has a maximum at about 450 nm characteristic for silver particles with a widely distributed size (20–80 nm) as has been shown in AFM images [22,23,25,26]. The absorption spectrum of SCCS shows irregular shape and indicates the presence of rod-like particles, probably aggregates of few individual colloids. This particular absorption shape was achieved for the described above preparation which we found to be highly reproducible. There is also possible to deposit “thinner” colloids without elongated particles which show more regular absorption [18]. A strong enhancement property we believe are attributed to SCCS with preparation described above.

Labeled-Protein Deposition

700 μ L of 10 μ M FITC-HSA ($L = 9$, Sigma-Aldrich) or Texas Red-BSA ($L = 3.5$, Molecular Probes; where L is the molar ratio of fluorophore to protein molecule) solution in 0.01 \times PBS was deposited on each quartz slide (45 \times 12.5 mm, half coated with SIF or SCCS) and placed in humid chamber at 5°C overnight. Next, slides were washed 3 times with 0.01 \times PBS and covered with one part of 0.5 mm demountable cuvette filled up with 0.01 \times PBS. In this procedure the homogenous protein monolayer, covered equally silvered and unsilvered area was obtained [27].

Fluorescence Measurements

All measurements were performed using front-face geometry in a 0.5 mm demountable cuvettes. Emission spectra were measured using an SLM 8000 spectrofluorometer. For the time-resolved frequency-domain measurements, the 514 nm excitation was obtained from a mode-locked argon ion laser, 76 MHz repetition rate. The emission was observed through a combination of holographic super-notch plus (Kaiser Optical System, Inc. Ann Arbor, MI) filter and a 540 nm interference filter for fluorescein or 620 nm interference filter for Texas Red, which reduced scattered and/or background to less than 1% of the sample signal. Excitation and emission polarizers were oriented vertically and 54.7° from the vertical, respectively.

The FD intensity decay were measured using 10 GHz fluorometer [28] and analyzed in terms of the multi-exponential model

$$I(t) = \sum_i \alpha_i \exp(-t/\tau_i) \quad (1)$$

where τ_i are the lifetimes with amplitudes α_i and $\sum \alpha_i = 1.0$. The contribution of each component to the steady state intensity is given by

$$f_i = \frac{\alpha_i \tau_i}{\sum_j \alpha_j \tau_j} \quad (2)$$

where the sum in the denominator is over all the decay times and amplitudes. The mean decay time is given by

$$\bar{\tau} = \sum_i f_i \tau_i \quad (3)$$

The amplitude-weighted lifetime is given by

$$\langle \tau \rangle = \sum_i \alpha_i \tau_i \quad (4)$$

Results and Discussion

Emission Spectra of TR-BSA

Emission spectra of Texas Red labeled bovine serum albumin, $L = 3.5$ (TR-BSA) deposited on SCCS and SIFs are presented in Fig. 2. The spectra were measured at the same illumination and detection conditions which allows a direct comparison. Whereas the intensities measured on unsilvered areas of slides were similar, the emission on SCCS (Fig. 2, bottom) was about twice stronger than on SIFs (Fig. 2, top). For comparison we present also the emission spectrum of the yellow part of the colloid coated slide (Fig. 2, middle). The fluorescence enhancement, defined as a ratio of intensities detected on silvered/unsilvered slides, was in the case of SCCS about 16 and the observed emission is visually brighter than on SIFs.

The increase of the brightness observed on silvered part of the slides is a result of two possible processes: 1) an increase of a local field near the metal particles and 2) an increase of radiative decay rate Γ [25,26,29,30]. The local field enhancement provides a higher excitation rate but does not alter the lifetime of fluorophore. This effect of metal particles on fluorophores is equivalent to the use of stronger illumination for the excitation process (Scheme 1). The second effect increases the quantum yield of the fluorophore. According to the Scheme 1, in absence of metal, the quantum yield (Φ) equals:

$$\Phi = \frac{\Gamma_m}{k_{nr} + \Gamma} \quad (5)$$

whereas in presence of metal

$$\Phi_m = \frac{\Gamma_m}{k'_{nr} + \Gamma_m} \quad (6)$$

A higher value of radiative decay rate (Γ_m) results in a higher quantum efficiency. Of course, Φ_m can not exceed 1.0, therefore the increase in brightness due to increase of radiative decay rate can be maximally $1.0/\Phi$. The quantum yield of TR-BSA ($L = 3.5$) is about 0.2, therefore the increase of radiative decay and eventual dequenching can be responsible only for a factor of 5 in increased brightness. The remaining factor of about 3 is due to enhanced local field. However, there is not significant self-quenching in TR-BSA at labeling 3.5. Stronger self-quenching for highly labeled protein will be discussed later in the section Fluorescence Enhancement of Highly Labeled FI-HSA.

Lifetimes of TR-BSA

Usually, an increase in quantum yield corresponds to the increase of lifetime. This is because in most conventional experiments the non-radiative decay rate is being manipulated and often the changes in lifetimes can be replaced with changes in quantum yields (Stern-Volmer quenching or energy transfer for example). Simultaneous observation of increased quantum yield and decreased lifetimes is possible only if there is an increase in the radiative decay rate. For the lifetimes, according to Scheme 1 in absence of metal we have:

$$\tau = \frac{1}{k_{nr} + \Gamma} \quad (7)$$

and in the presence of metal particles:

$$\tau = \frac{1}{k'_{nr} + \Gamma_m} \quad (8)$$

We measured the intensity decays of TR-BSA when deposited on unsilvered and silvered slides (Fig. 3). The amplitude averaged lifetime of TR-BSA on SIFs (Fig. 3, bottom) is about 5-fold shorter than on quartz (Fig. 3, top). Still shorter lifetime has been observed on SCCS (Fig. 3, middle). This indicates that on SCCS there is a stronger increase in radiative decay rate than on SIFs. The analysis of intensity decays (Table I) shows the presence of a long component in

the case of SIFs (Table I, τ_3) which is absent for SCCS. The long component in the intensity decay can originate from the not affected species e.a. proteins deposited outside of effective enhancement distance from silver particles.

Photostability of TR-BSA

We observed a time dependent emission of TR-BSA deposited on unsilvered and silvered slides upon a continuous illumination from argon ion laser (~ 20 mW, 514 nm focused to a spot with diameter of about $50 \mu\text{m}$) (Fig. 4.). The excitation intensity was held constant. At these conditions the photodegradation ratio is about the same for SIFs, SCCS and unsilvered quartz slides. However, the amount of photons (proportional to the area under curve) detected within 5 min from silvered slides is much higher than from unsilvered slides. In order to obtain the same amount of photons from silvered slide as from unsilvered, the excitation intensity can be many fold reduced. We already have shown that the comparison of photostabilities when normalized to the same initial intensity always favored silvered slides [13,15–22].

There are two opposite factors affecting the photostability. First, the enhanced local field will result in increased photobleaching. Second, the decreased lifetime of the fluorophore will increase the photostability since the molecules will spend less time in the excited state. The observed dependence (Fig. 4) is a composition of all these factors.

Fluorescence Enhancement of Highly Labeled FI-HSA

Next, we extended the comparison of SIFs and SCCS on highly labeled protein where self-quenching is significant. The fluorescein intensity and lifetime of highly labeled HSA is strongly quenched, which make such probes less useful in microscopy, spectroscopy, and diagnostics. The interaction of excited fluorescein molecules with silver particles appears to compete with the interaction between fluoresceins, resulting in the release of self-quenching. The measured enhancements on silvered slides are larger from the highly labeled system (Fig. 5). For FI-HSA ($L = 9$) the measured enhancements are 12.8 and 36-fold for SIFs and SCCS, respectively. The enhancement on SIFs is slightly lower than reported previously [30] for FI-HSA ($L = 9$). This small discrepancy can be due to SIFs preparation. The observed enhancement of 36-fold for highly labeled FI-HSA ($L = 9$) is more than twice higher than for low labeled TR-BSA. Assuming similar local field enhancement and a similar increase in radiative rate, the nonradiative rate (Scheme 1) appear to decrease two fold on SCCS, comparing to the quartz. In fact, the amplitude averaged lifetime changes stronger in absence of self-quenching (Fig. 6, Table I). The ratio of $\langle \tau \rangle$ in the presence of SCCS for TR-BSA is about 20 and for FI-HSA is only 9.

Conclusions

The presence of silver particles significantly increases the brightness of deposited labeled proteins. The enhancement is stronger for highly labeled system due to a partial release of self-quenching. The lifetimes of the labeled proteins are much shorter on silver particles than on quartz substrate. The comparison of enhancements observed on SIFs and SCCS favors the latter. In addition to two-fold higher enhancements the intensity decays observed on SCCS do not contain a long component. Both, SIFs and SCCS are relatively easy to prepare and the preparation is highly reproducible. We believe that silvered surfaces will find use in modern sensing technologies such as immunoassays and DNA arrays.

Acknowledgments

This work was supported by NIH National Center for Research Resource, RR-08119, the Human Genome Institute, HG-002655, and from the National Institute for Bioimaging and Bioengineering, NIH-EB00682 and EB-00980.

References

1. Drexhage, KH. Progress in Optics. Wolfe, E., editor. North Holland, Amsterdam: 1974. p. 161-232.
2. Amos RM, Barnes WL. Modification of the spontaneous emission rate of Eu^{3+} ions close to a thin metal mirror. *Phys Rev B* 1997;55(11):7249–7254.
3. Hinds EA. Cavity quantum electrodynamics. *Adv At Mol Opt Phys* 1991;28:237–289.
4. Haroche S, Kleppner D. Cavity quantum electrodynamics. *Phys Today* 1989:24–30.
5. Haroche S, Raimond JM. Cavity quantum electrodynamics. *Sci Am* 1993;268(4):54–62.
6. Michaels AM, Jiang J, Brus L. Ag nanocrystal junctions as the site for surface-enhanced Raman scattering of single rhodamine 6G molecules. *J Phys Chem B* 2000;104:11965–11971.
7. Freeman RG, Graber KC, Allison KJ, Bright RM, Davis JA, Guthrie AP, Homme MB, Jackson MA, Smith PC, Walter DG, Natan MJ. Self-assembled metal colloid monolayers: An approach to SERS substrates. *Science* 1995;267:1629–1632. [PubMed: 17808180]
8. Weitz DA, Garoff S, Anson CD, Gramila TJ. Fluorescent lifetimes of molecules on silver-island films. *Opt Lett* 1982;7(2):89–91. [PubMed: 19710833]
9. Aussenegg FR, Leitner A, Lippitch ME, Reinisch H, Reigler M. Novel aspects of fluorescence lifetime for molecules positioned close to metal surface. *Surface Sci* 1987;139:935–945.
10. Leitner A, Lippitch ME, Draxler S, Riegler M, Aussenegg FR. Fluorescence properties of dyes absorbed to silver islands, investigated by picosecond techniques. *Appl Phys B* 1985;36:105–109.
11. Gersten J, Nitzan A. Spectroscopic properties of molecules interacting with small dielectric particles. *J Chem Phys* 1981;75(3):1139–1152.
12. Weitz DA, Garoff S, Gersten JI, Nitzan A. The enhancement of Raman scattering, resonance Raman scattering, and fluorescence from molecules absorbed on rough silver surface. *J Chem Phys* 1983;78(9):5324–5338.
13. Gryczynski I, Malicka J, Shen Y, Gryczynski Z, Lakowicz JR. Multiphoton excitation of fluorescence near metallic particles: Enhanced and localized excitation. *J Phys Chem B* 2002;106:2191–2195.
14. Wenseleers W, Stellacci F, Meyer-Friedrichsen T, Mangel T, Bauer CA, Pond SJK, Marder SR, Perry JW. Five orders-of-magnitude enhancement of two-photon absorption for dyes on silver nanoparticle fractal clusters. *J Phys Chem B* 2002;106:6853–6863.
15. Maliwal BP, Malicka J, Gryczynski I, Gryczynski Z, Lakowicz JR. Fluorescence properties of labeled proteins near silver colloid surfaces. *Biopolymers* 2003;70:585–594. [PubMed: 14648768]
16. Geddes CD, Parfenov A, Roll D, Gryczynski I, Malicka J, Lakowicz JR. Roughened silver electrodes for use in metal-enhanced fluorescence. *Spectrochim Acta A*. in press
17. Geddes CD, Parfenov A, Lakowicz JR. Photodeposition of silver can result in metal-enhancement fluorescence. *Appl Spectr* 2003;57:526–531.
18. Geddes CD, Cao H, Gryczynski I, Gryczynski Z, Lakowicz JR. Metal-enhanced fluorescence (MEF) due to silver colloid on a planar surface: Potential applications of indocyanine green to in vivo imaging. *J Phys Chem A* 2003;107:3443–3449.
19. Geddes CD, Parfenov A, Roll D, Gryczynski I, Malicka J, Lakowicz JR. Silver fractal-like structures for metal-enhanced fluorescence: Enhanced fluorescence intensities and increased probe photostabilities. *J Fluoresc* 2003;13(3):267–276.
20. Parfenov A, Gryczynski I, Malicka J, Geddes CD, Lakowicz JR. Enhanced fluorescence from fluorophores on fractal silver surfaces. *J Phys Chem B* 2003;107:8829–8833.
21. Malicka J, Gryczynski I, Lakowicz JR. DNA hybridization assays using metal-enhanced fluorescence. *Biochem Biophys Res Commun* 2003;306:213–218. [PubMed: 12788090]
22. Malicka J, Gryczynski I, Fang J, Lakowicz JR. Photostability of Cy3 and Cy5-labeled DNA in the presence of metallic silver particles. *J Fluoresc* 2002;12:439–447.
23. Geddes CD, Parfenov A, Roll D, Fang J, Lakowicz JR. Electrochemical and laser deposition of silver for use in metal-enhanced fluorescence. *Langmuir* 2003;19:6236–6241.
24. Lee PC, Meisel D. Adsorption and surface-enhanced Raman of dyes on silver and gold sols. *J Phys Chem* 1982;86:3391–3395.
25. Lakowicz JR. Radiative decay engineering: Biophysical and biomedical applications. *Anal Biochem* 2001;298:1–24. [PubMed: 11673890]

26. Lakowicz JR, Shen Y, D'Auria S, Malicka J, Fang J, Gryczynski Z, Gryczynski I. Radiative decay engineering. 2. Effects of silver island films on fluorescence intensity, lifetimes, and resonance energy transfer. *Anal Biochem* 2002;301:261–277. [PubMed: 11814297]
27. Malicka J, Gryczynski I, Gryczynski Z, Lakowicz JR. Effects of fluorophore-to-silver distance on the emission of cyanine-dye-labeled oligonucleotides. *Anal Biochem* 2003;315:57–66. [PubMed: 12672412]
28. Laczko G, Lakowicz JR, Gryczynski I, Gryczynski Z, Malak H. A10-GHz frequency-domain fluorometer. *Rev Sci Instrum* 1990;61:233–237.
29. Kummerlen J, Leitner A, Brunner H, Aussenegg FR, Wokaun A. Enhanced dye fluorescence over silver island films: Analysis of the distance dependence. *Mol Phys* 1993;80(5):1031–1046.
30. Lakowicz JR, Malicka J, D'Auria S, Gryczynski I. Release of the self-quenching of fluorescence near silver metallic surfaces. *Anal Biochem* 2003;320:13–20. [PubMed: 12895465]

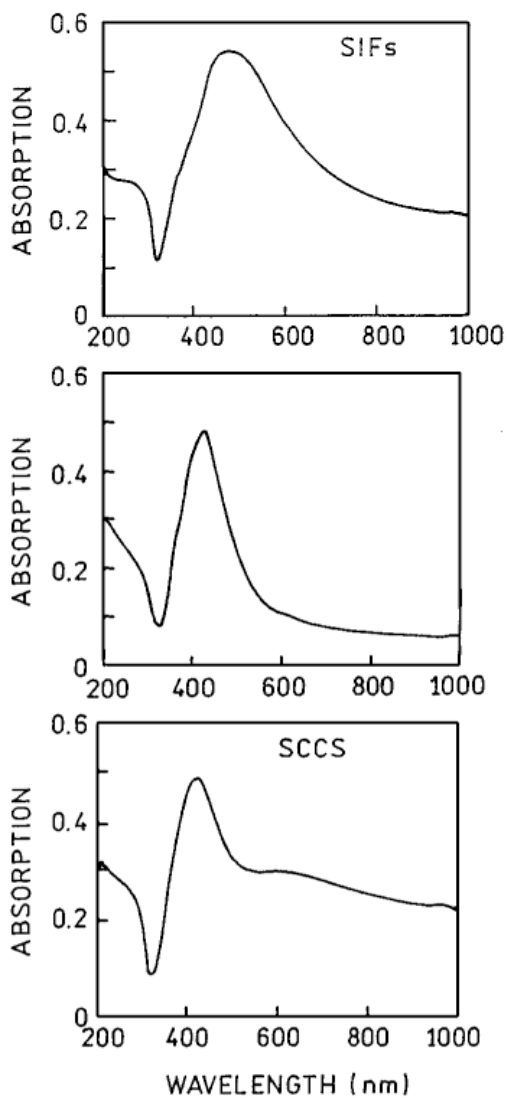


Fig. 1. Absorption spectra of silver island film, SIFs (top), yellow part (middle) and silver colloid coated surface, SCCS (bottom).

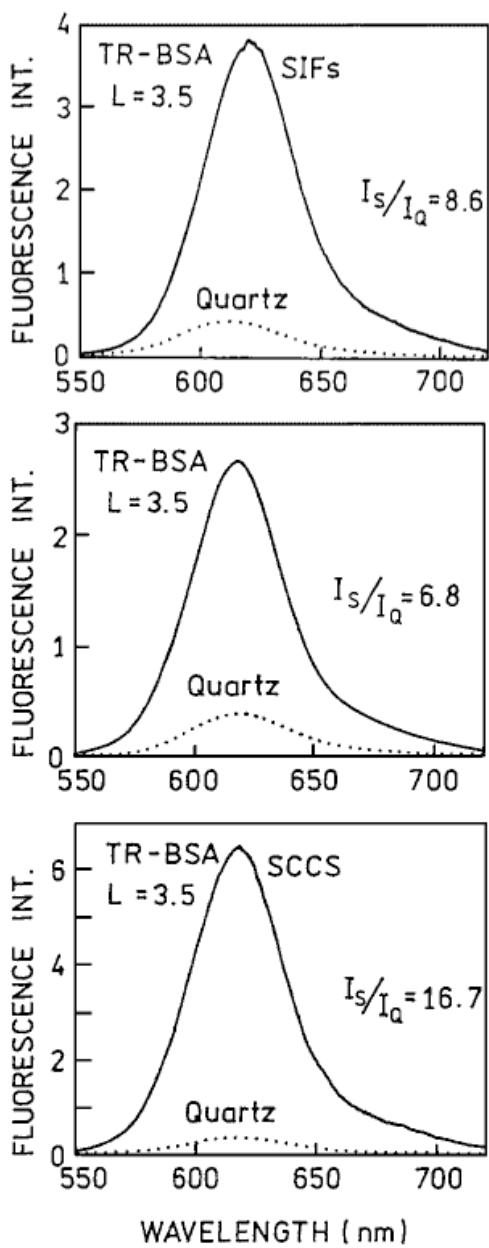


Fig. 2. Emission spectra of Texas Red labeled BSA (TR-BSA) measured for SIFs (top), yellow part (middle) and SCCS (bottom).

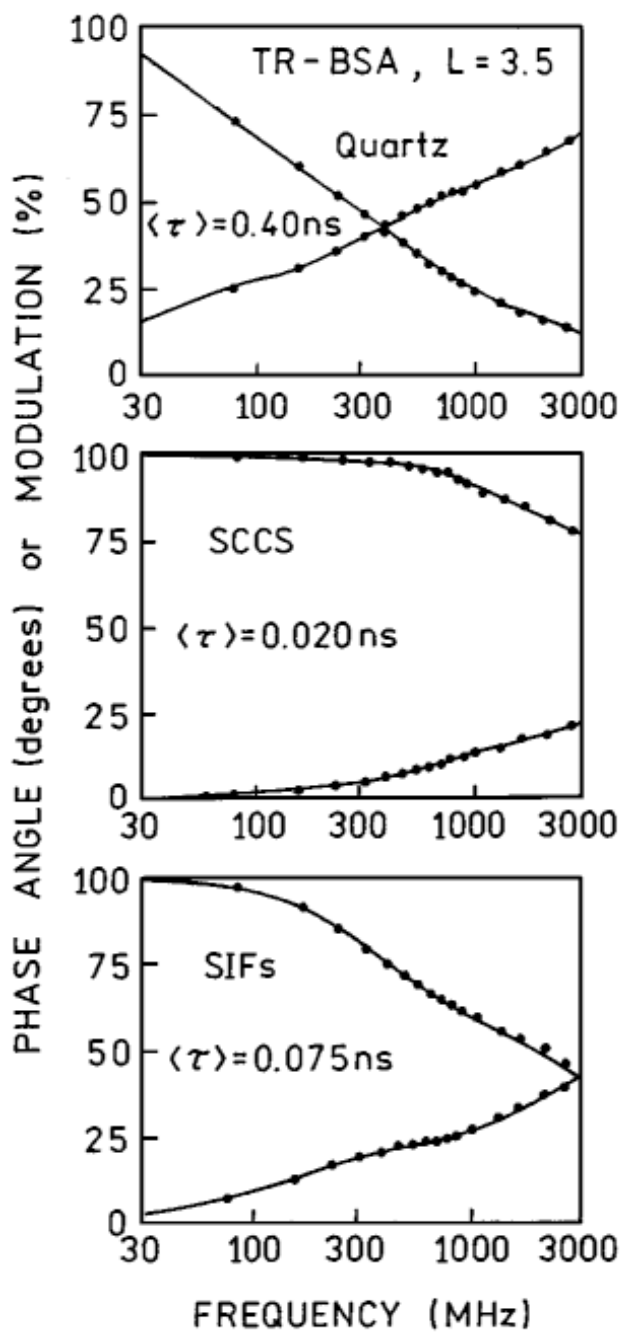


Fig. 3. Frequency-domain lifetimes for TR-BSA deposited on quartz (top), colloid coated surface (middle) and SIFs (bottom). The amplitude averaged lifetimes are 2–3 fold shorter on colloid coated surface than on SIFs.

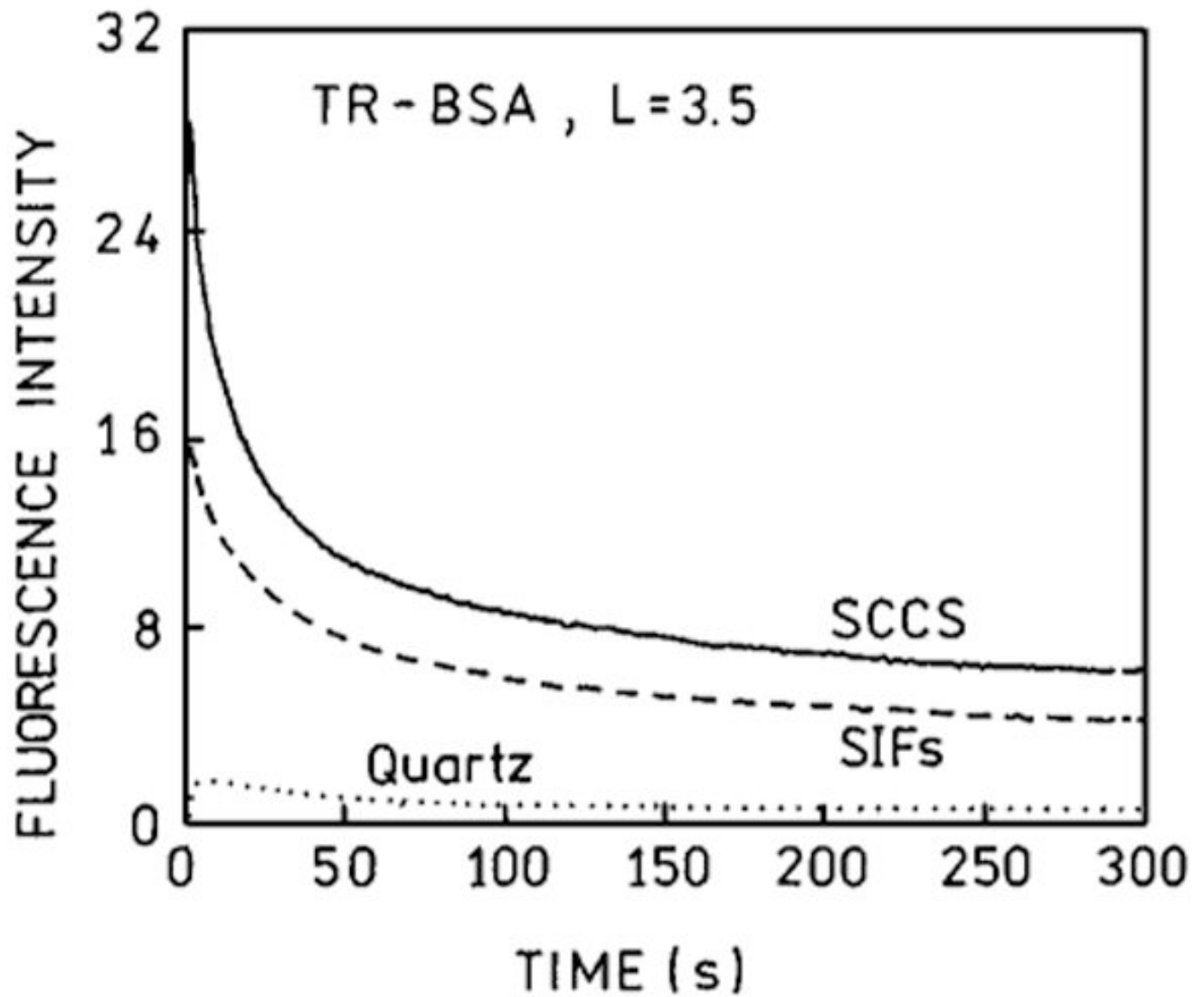


Fig. 4. Photostabilities of TR-BSA on quartz (···), SIFs (---) and SCCS (—) measured at the same excitation and observation conditions.

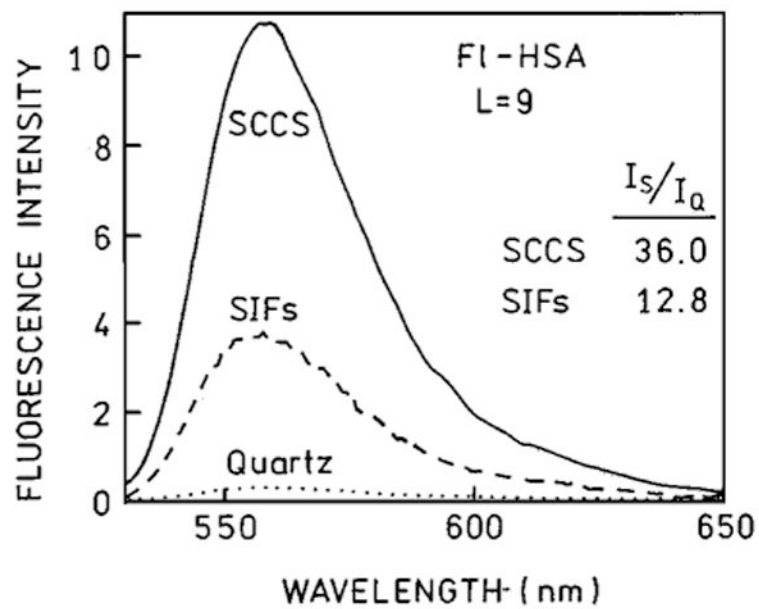


Fig. 5. Emission spectra of FI-HSA ($L = 9$) measured on quartz (\cdots), SIFs ($---$) and SCCS ($---$). The experimental conditions were kept constant.

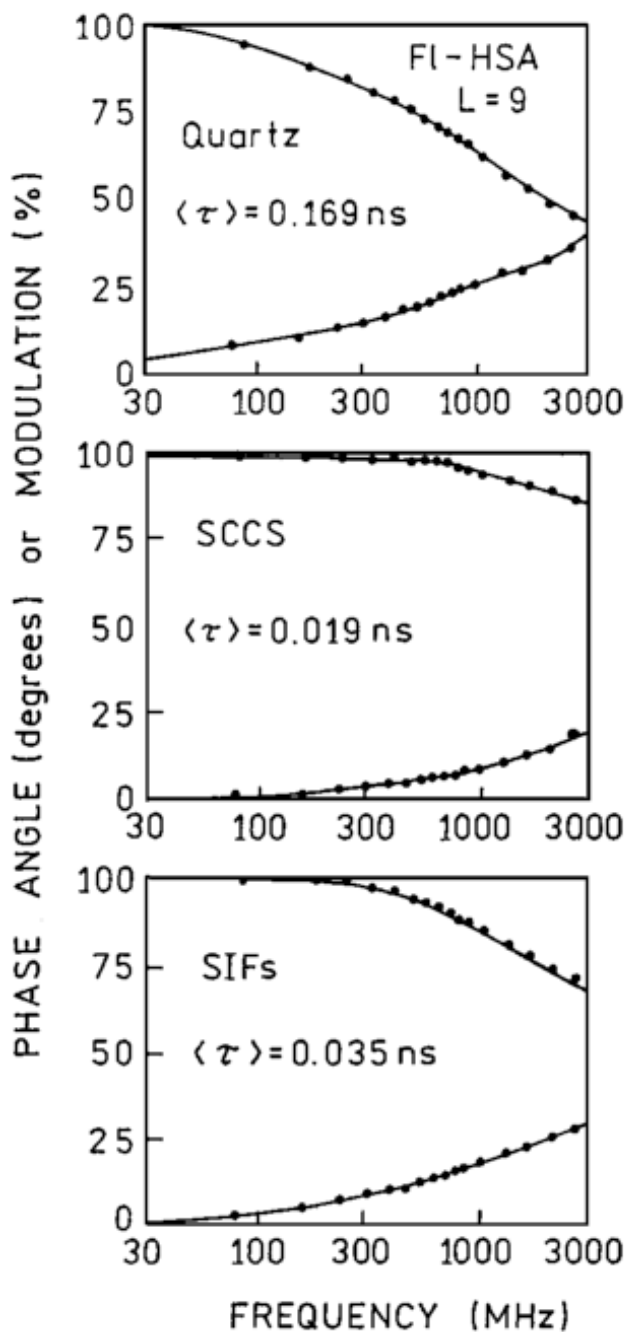
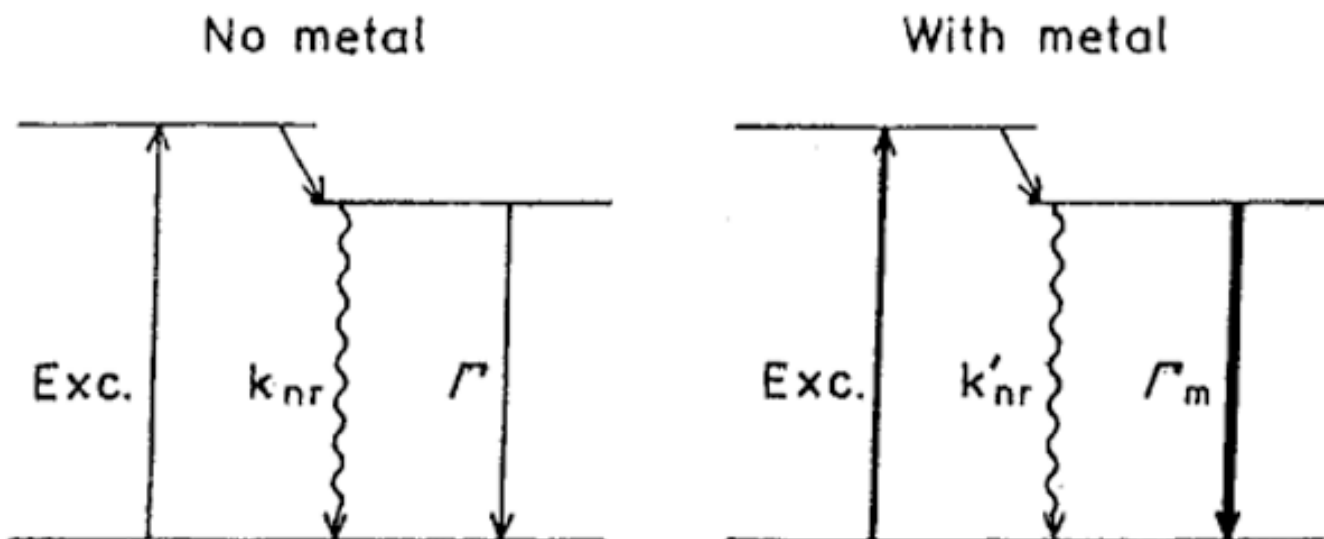


Fig. 6. Frequency-domain lifetimes of fluorescein in highly labeled HSA deposited on quartz (top), colloid coated surface (middle) and SIFs (bottom).

**Scheme 1.**

Simplified Jablonski diagram for free (left) and metal affected molecules (right). Due to the coupling of fluorophore excited dipole to the metal particle the radiative decay rate increases ($\Gamma_m \gg \Gamma$). In the case of significant self-quenching the non-radiative rate can decrease in presence of metal ($k'_{nr} < k_{nr}$). The enhanced local field is indicated as a thicker excitation (right).

Table I
Multi-exponential Analysis of TR-BSA Intensity Decays

Compound/conditions	$\langle \tau \rangle$ (ns)	$\bar{\tau}$ (ns)	a_1	τ_1 (ns)	a_2	τ_2 (ns)	a_3	τ_3 (ns)	χ^2_R
TR-BSA, in buffer	2.44	3.59	0.428	0.490	0.572	3.89	—	—	2.0
TR-BSA, on quartz	0.397	1.69	0.595	0.083	0.345	0.46	0.060	3.15	1.4
TR-BSA, on SCCS	0.020	0.054	0.959	0.015	0.041	0.125	—	—	1.3
TR-BSA, on SIFs	0.075	0.293	0.836	0.036	0.117	0.128	0.047	0.64	2.6
Fl-HSA, in buffer	0.67	1.24	0.285	0.189	0.611	0.593	0.104	2.40	1.4
Fl-HSA, on quartz	0.169	0.394	0.007	0.031	0.876	0.206	0.117	1.61	1.7
Fl-HSA, on SCCS	0.019	0.019	1.0	0.019	—	—	—	—	1.2
Fl-HSA, on SIFs	0.077	0.035	0.948	0.026	0.052	0.199	—	—	2.5